

Formation of regular black hole from baryonic matter

Vitalii Vertogradov,^{1,2,*} Ali Övgün,^{3,†} and Daniil Shatov^{1,‡}

¹*Physics department, Herzen state Pedagogical University of Russia,
48 Moika Emb., Saint Petersburg 191186, Russia*

²*SPB branch of SAO RAS, 65 Pulkovskoe Rd, Saint Petersburg 196140, Russia*

³*Physics Department, Eastern Mediterranean University,
Famagusta, 99628 North Cyprus, via Mersin 10, Turkiye.*

(Dated: February 4, 2025)

We investigate regular black hole formation through the gravitational collapse of baryonic matter characterized by a time- and radius-dependent coefficient of equation of state. Our analysis yields exact solutions to Einstein's field equations that describe singularity-free spacetimes. These solutions are matched to the Husain metric, providing a complete description of dynamical black holes with a barotropic equation of state. The solutions reveal interesting physical behavior but face important challenges: the pressure increases with radius and violates the dominant energy condition beyond a critical value, requiring external matching for a complete spacetime description. Our analysis of black hole shadows shows that both the shadow and photon sphere radii increase monotonically with the equation of state parameter α . The matching between interior and exterior solutions suggests a phase transition occurs during collapse, potentially delaying apparent horizon formation. This prediction, combined with distinct shadow characteristics, offers promising avenues for observational tests of regular black hole models.

PACS numbers: 95.30.Sf, 04.70.-s, 97.60.Lf, 04.50.Kd

Keywords: Black hole; Vaidya spacetime; Singularities; Dynamical spacetimes; Shadow.

I. INTRODUCTION

Penrose's singularity theorems demonstrate that apparent horizon formation inevitably leads to spacetime singularities [1, 2], highlighting a fundamental limitation of general relativity in describing physics at extreme gravitational scales [3]. The Event Horizon Telescope's groundbreaking observations of supermassive black holes in M87 and Sagittarius A* have transformed these theoretical objects into observable reality, bringing renewed urgency to the singularity problem [4–8]. However, the singularity theorems assume the strong energy condition - that gravity remains universally attractive. This assumption can be violated by exotic matter states, with dark energy serving as a cosmic-scale example of repulsive gravity. Such violations could potentially resolve the singularity problem by preventing the formation of infinite density states.

The concept that extremely dense matter might transition into a vacuum state resembling a de Sitter core was first proposed independently by Gliner [9] and Sakharov in 1966 [10]. This groundbreaking insight laid the foundation for understanding potential mechanisms to avoid singularities in black holes. Building on these ideas, Bardeen made a significant advance in 1968 by constructing the first explicit model of a nonsingular black hole [11]. However, a crucial question remained unresolved for nearly three decades: what type of matter could physically support such a regular center? This theoretical puzzle was finally addressed when Ayon-Beato and Garcia demonstrated that nonlinear electro-

dynamics could serve as the source for the Bardeen black hole, providing a concrete physical mechanism for singularity avoidance [12, 13].

Nonlinear electrodynamics as a mechanism for regular black hole formation faces fundamental challenges. The primary limitation stems from the non-uniqueness of the theory - there exists a vast family of nonlinear electromagnetic theories capable of generating regular centers, with no clear physical principle to select among them. This theoretical redundancy suggests that nonlinear electrodynamics may not provide the most fundamental explanation for singularity avoidance [14–18]. The existence of regular centers in black hole solutions has been established only under specific conditions: the presence of magnetic monopoles and the complete absence of electric charge. This constraint significantly restricts the physical applicability of these models, particularly given that magnetic monopoles remain unobserved in nature [19–21]. Regular black holes supported by nonlinear electrodynamics rely on charge as a key parameter for regularization. However, real astrophysical black holes are generally considered to be electrically neutral. Even if a regular center were to form, it would likely be transient, as a singularity would inevitably develop due to the charged Penrose process [22–24] or through the accretion of matter onto the black hole.

Another fundamental challenge is understanding the formation of regular black holes. While a regular center necessitates the presence of exotic matter, regular stars are composed of ordinary baryonic matter. Consequently, during gravitational collapse, ordinary matter would have to undergo a transformation into an exotic form capable of preventing singularity formation. A recent model [25] describes the gravitational collapse of dust and radiation, where dust transitions into a radiation process that intensifies near the

* vvertogradov@gmail.com

† ali.ovgun@emu.edu.tr

‡ shatov.ddb@mail.ru

centerpotentially facilitating the formation of a regular core. Additionally, previous studies have explored the gravitational collapse of dust leading to the emergence of regular black holes [26]. Numerous studies have been dedicated to investigating the properties of static and stationary regular black holes [27–68] (see [69, 70] for a comprehensive review and references therein). However, comparatively fewer studies have focused on the problem of their formation [14, 70–75].

In this work, we investigate the gravitational collapse of baryonic matter characterized by a dynamical equation of state with time- and radius-dependent coefficients. Through rigorous analysis of Einstein’s field equations, we obtain a family of solutions describing regular black holes - spacetimes free from central singularities. Our solutions provide a unified framework that captures both the formation mechanism of black holes through gravitational collapse and their subsequent evolution through Hawking evaporation.

By establishing an exact matching with metrics describing collapsing baryonic matter, we construct a comprehensive physical model that traces the complete life cycle of regular black holes from their formation to their eventual fate. This matching procedure ensures the physical consistency of our solutions while illuminating the detailed dynamics of gravitational collapse. Additionally, we analyze the distinctive shadow characteristics of these regular black holes, deriving specific observational signatures that could potentially distinguish them from their singular counterparts in future astronomical observations.

The paper is organized in a systematic progression through the theoretical framework and its applications. In Section 2, we establish the mathematical foundations of regular black holes, presenting the general formalism that underpins our analysis. This section develops the necessary field equations and derives novel solutions to Einstein’s equations that characterize regular black holes with well-defined properties. Section 3 advances the analysis by demonstrating the precise matching conditions between our derived solutions and the Hussain metric, ensuring mathematical consistency and physical relevance. Section 4 explores the observable implications of these solutions through a detailed investigation of black hole shadow characteristics. The final two sections synthesize our findings: Section 5 presents a comprehensive discussion of the theoretical results and their physical implications, while Section 6 concludes with broader insights into the significance of our work and suggests promising directions for future research.

We use a geometrized system of units in which $c = 8\pi G = 1$. Also, we adopt the signature $-+++$.

II. GENERAL APPROACH

In this section, we briefly examine the conditions required for the formation of a regular black hole. We derive a general formula and identify the criteria under which a regular black hole can emerge from gravitational collapse, considering an arbitrary equation of state. To begin, we analyze a metric that represents the most general form of a spherically

symmetric dynamical black hole, expressed as:

$$ds^2 = - \left(1 - \frac{2M(v, r)}{r} \right) dv^2 + 2\varepsilon dvdr + r^2 d\Omega^2. \quad (1)$$

Here, $M(v, r)$ is the mass function, which depends on both the advanced time v and the radial coordinate r . This function characterizes the dynamical nature of the black hole, allowing for variations in mass due to processes such as accretion or radiation. The parameter $\varepsilon = \pm 1$ indicates the direction of the radiation flow, where $\varepsilon = +1$ corresponds to ingoing radiation and $\varepsilon = -1$ corresponds to outgoing radiation. The coordinate v represents the advanced time in Eddington-Finkelstein coordinates, which are particularly useful for describing causal structures, such as light rays near the horizon. The angular part of the metric is given by $d\Omega^2 = d\theta^2 + \sin^2\theta d\varphi^2$, which describes the geometry of a unit two-sphere. This metric setup is essential for studying regular black holes, as it provides a general framework to analyze the radial and time-dependent evolution of the system. Its generality makes it applicable to a wide range of scenarios, including gravitational collapse, black hole evaporation, and the effects of exotic matter fields [76–85].

The metric in Eq. (1) is supported by an energy-momentum tensor of the form:

$$T_{ik} = (\rho + P)(l_i n_k + l_k n_i) + P g_{ik} + \mu l_i l_k, \quad (2)$$

where ρ and P denote the energy density and pressure of the matter, respectively. The parameter $\mu = \varepsilon \frac{2M}{r^2}$ represents the total energy flux. The vectors l^i and n^i are null vectors with the following properties:

$$\begin{aligned} l_i &= \delta_i^0, \\ n_i &= \frac{1}{2} \left(1 - \frac{2M}{r} \right) \delta_i^0 - \varepsilon \delta_i^1, \\ l^i l_i &= n^i n_i = 0, \quad l^i n_i = -1. \end{aligned} \quad (3)$$

The energy density ρ and pressure P for this spacetime are given as follows:

$$\begin{aligned} \rho &= \frac{2M'}{r^2}, \\ P &= -\frac{M''}{r}. \end{aligned} \quad (4)$$

The system of equations (4) consists of two differential equations and three unknown functions: $\rho(v, r)$, $P(v, r)$, and $M(v, r)$. Therefore, an additional equation must be introduced to close the system, providing three equations for the three unknown functions.

A common approach to close the system is by introducing an equation of state (EoS), which establishes a relationship between the energy density and pressure, typically expressed as $P = P(\rho)$. One of the simplest and widely used forms is the barotropic equation of state, where the pressure is linearly related to the energy density as $P = k\rho$.

The parameter k in this relation determines the type of matter described by the equation of state. For example:

- $k = 1$: Stiff fluid, often used to describe highly compressed matter.
- $k = \frac{1}{3}$: Electromagnetic radiation, consistent with a relativistic gas or radiation-dominated era.
- $k = 0$: Dust, corresponding to pressureless matter.
- $k = -1$: Vacuum energy, representing dark energy or a cosmological constant.

In the context of gravitational collapse, it is expected that the matter undergoes changes in its equation of state during different stages of the collapse. This implies that the parameter k should depend on both the radius r and the time v , reflecting the evolving properties of the collapsing matter. Consequently, the equation of state takes the generalized form:

$$P = k(v, r)\rho. \quad (5)$$

where $k(v, r)$ is now a function of both the radial coordinate and time, capturing the dynamic and spatial variations of the matter properties during the collapse. This generalization allows the system to account for transitions between different phases of matter and provides a more realistic description of gravitational collapse and the potential formation of regular black holes.

From Eq. (4), the following relationship between pressure and energy density can be obtained:

$$P = -\rho - \frac{r}{2}\rho'. \quad (6)$$

or

$$\rho'r = -2P - 2\rho \quad (7)$$

denotes the radial derivative of the energy density. Substituting this expression into the equation of state $P = k\rho$, one obtains:

$$\rho'r = -(2 + 2k)\rho. \quad (8)$$

The solution of this differential equation is given by:

$$\rho = \frac{\rho_0}{r^2} e^{-\int \frac{2k}{r} dr}. \quad (9)$$

here ρ_0 is a positive integration constant. This solution represents the energy density ρ as a function of the radial coordinate r , and its behavior depends on the form of $k = k(v, r)$. To ensure a regular solution at the center ($r \rightarrow 0$), the parameter k is expanded as a power series around $r = 0$:

$$k = \sum_{i=0}^n k_i r^i. \quad (10)$$

where the coefficients $k_i(v)$ are functions of the advanced time v and are defined as:

$$k_i(v) \equiv \left. \frac{1}{i!} \frac{\partial^i k}{\partial x^i} \right|_{r=0}. \quad (11)$$

then (9) can be written as

$$\rho = \frac{\rho_0}{r^{2+2k_0}} e^{-2\sum_{i=1}^n k_i \frac{r^i}{i}}. \quad (12)$$

To ensure a regular center, it is necessary to demand that $\rho(0) = \rho_0 = \text{const.}$, meaning the energy density must remain finite at the center. This requirement imposes the following constraint on the parameter k_0 :

$$k_0 \leq -1. \quad (13)$$

If $k_0 = -1$, the center corresponds to a vacuum medium with a de Sitter core. On the other hand, if $k_0 < -1$, the energy density vanishes, and the central region transitions to a Minkowski spacetime, indicating an absence of matter. Using Eq. (9), the mass function can be derived in the following general form:

$$M(v, r) = \frac{\rho_0}{2} \int r^{-2k_0} e^{-2\sum_{i=1}^n k_i \frac{r^i}{i}} + M_0(v). \quad (14)$$

where $M_0(v)$ is an integration function depending on the advanced time v . This function represents the dynamic contribution to the mass function from the evolving system.

One critical property of a regular center is that the mass function must vanish at the center, i.e., $M(v, 0) = 0$. To satisfy this condition and eliminate $M_0(v)$, it must hold that:

$$\lim_{r \rightarrow 0} \frac{\rho_0}{2} \int r^{-2k_0} e^{-2\sum_{i=1}^n k_i \frac{r^i}{i}} = -M_0(v) \quad (15)$$

implying no additional contributions to the mass at the center. This ensures the consistency of the regular center condition and provides a physically meaningful mass function.

A. Model 1: $k_0 = -1, k_3 = k_3(v)$

The integral in the formula (14) simplifies only for a specific set of parameters k_i . Among these cases, we are particularly interested in regular solutions with a de Sitter core at the center. Such solutions correspond to cases where the parameter choices allow for a finite energy density and a well-defined spacetime structure at the core. Notably, only a few parameter configurations result in a tractable form for the mass function.

In this study, we focus on the simplest case where $k_1 = k_2 = 0$. This choice eliminates the higher-order terms in the expansion of $k(v, r)$, significantly simplifying the calculation. By applying the method described in the previous section, the mass function can be expressed as:

$$M(v, r) = \frac{\rho_0(v)}{2} \int e^{-2\int \frac{k(v,r)}{r} dr} dr + M_0(v), \quad (16)$$

where $\rho_0(v)$ is the central energy density as a function of advanced time v , and $M_0(v)$ is an additional integration function of v , representing the overall black hole mass. The term $M_0(v)$ is typically determined by boundary conditions or asymptotic properties of the black hole.

This formulation emphasizes the role of $k(v, r)$ in defining the structure of the mass function and ensures that the solution remains regular at the center. The case $k_1 = k_2 = 0$ is particularly relevant as it corresponds to a de Sitter core, which is a common feature in regular black hole models, providing a smooth and nonsingular interior spacetime. After calculating the Kretschmann scalar for the generalized Vaidya spacetime, it is expressed as:

$$K = \frac{4}{r^6} [4(3M^2 - 4rMM' + 2r^2M'^2) + 4r^2M''(M - rM') + 4r^4M''^2], \quad (17)$$

where $M = M(v, r)$ is the mass function, $M' = \frac{\partial M}{\partial r}$, and $M'' = \frac{\partial^2 M}{\partial r^2}$.

To ensure regularity at the center ($r \rightarrow 0$), we require that the Kretschmann scalar remains finite:

$$\lim_{r \rightarrow 0} K \neq \infty. \quad (18)$$

This condition ensures that there are no curvature singularities at the center. Substituting the series expansion for $k(v, r)$ into the mass function $M(v, r)$ (from Eq. (16)) and the Kretschmann scalar K , we find that the coefficients $k_i(v)$ must satisfy certain constraints to ensure the finiteness of K as $r \rightarrow 0$.

Specifically, the following condition must hold:

$$M_0(v) = -\lim_{r \rightarrow 0} \frac{\rho_0(v)}{2} \int e^{-2 \int \frac{k(v,r)}{r} dr} dr, \quad (19)$$

where $M_0(v)$ is the integration function related to the black hole mass. This constraint ensures that the central mass contribution is well-defined and eliminates divergences in the Kretschmann scalar at the center. The condition ties the behavior of the coefficients $k_i(v)$ in the expansion of $k(v, r)$ to the structure of the spacetime, providing a consistent framework for describing regular black holes.

We begin by assuming the following specific parameter choices:

$$\begin{aligned} k_0(v) &= -1, \\ k_3(v) &= k_3(v), \\ k_1(v) &= k_2(v) = 0. \end{aligned} \quad (20)$$

With these assumptions, the mass function takes the form:

$$M(v, r) = M_0(v) - \frac{3\rho_0(v)}{2k_3(v)} e^{-\frac{1}{3}k_3(v)r^3}. \quad (21)$$

Now we consider different cases of $M_0(v)$:

- **Case 1:** $M_0(v) \equiv \frac{3\rho_0(v)}{2k_3(v)}$:

In this case, the spacetime described by the metric (1) with the mass function (21) represents a regular black hole, which is a dynamical generalization of the well-known Dymnikova regular black hole [86].

The Kretschmann scalar for this spacetime at $r = 0$ is given by:

$$\lim_{r \rightarrow 0} K = \frac{32}{27} M_0(v)^2 k_3(v)^2. \quad (22)$$

This ensures that the spacetime curvature at the center remains finite, consistent with the requirements of a regular black hole.

For this model, the energy density ρ and pressure P are expressed as:

$$\begin{aligned} \rho &= \frac{2}{3} M_0(v) k_3(v) e^{-\frac{1}{3}k_3(v)r^3}, \\ P &= \frac{2}{3} M_0(v) k_3(v) e^{-\frac{1}{3}k_3(v)r^3} \left(\frac{k_3(v)r^3}{6} - 1 \right). \end{aligned} \quad (23)$$

These expressions reveal the distribution of matter and its dynamics in the spacetime. The exponential term ensures that both the energy density and pressure decay smoothly away from the center, contributing to the regularity of the black hole.

The weak and dominant energy conditions impose the following constraints on the parameters of the solution:

$$\rho_0(v) > 0, \quad (24)$$

$$r \leq \left(\frac{12}{k_3} \right)^{\frac{1}{3}}. \quad (25)$$

This solution exhibits a *de Sitter core* at the center ($r \rightarrow 0$) and approaches the *Schwarzschild limit* at infinity ($r \rightarrow \infty$).

For specific choices of the functions:

$$\begin{aligned} k_3(v) &= (\mu - v)^2, \\ \rho_0(v) &= \frac{2}{3} \lambda k_3(v) v, \end{aligned} \quad (26)$$

we can visualize the behavior of the spacetime by plotting the function $F(v, r) = 1 - \frac{2M(v, r)}{r} = 0$, which represents the horizon structure. In Figure 1, $F(v, r) = 0$ is plotted as $v(r)$, with parameters $\mu = 4$ and $\lambda = 1$. Then we also plot the graph of $\dot{M} = 0$ in Figure 2.

- **Case 2:** $M_0(v) \neq \frac{3\rho_0(v)}{2k_3(v)}$:

In this case, the spacetime described by the metric (1) with the mass function (21) corresponds to a *singular black hole*. The Kretschmann scalar diverges as $r \rightarrow 0$, indicating the presence of a curvature singularity at the center.

It is possible that during the evolution, the function $N(v) \equiv \frac{c_1(v)}{3f(v)} - c_2(v)$ becomes zero only at specific values of v , such as v_1, v_2, v_3, \dots . This implies that the system transitions between states with *regular* and *singular centers* at these moments in time. Such behavior was first described in [87].

In Figure 1, the apparent horizon behavior is illustrated. The first model (Eq. (21)) violates the null energy condition

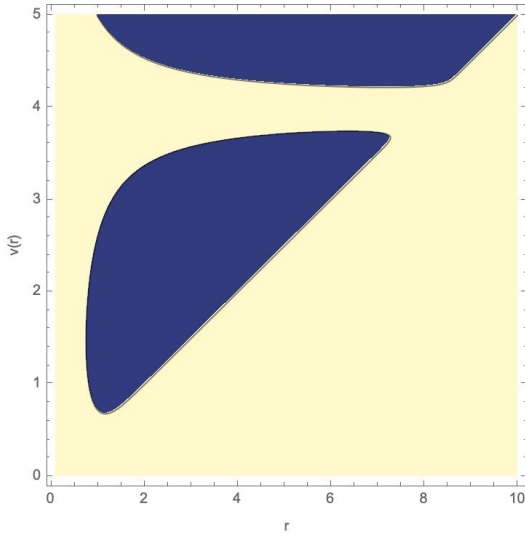


FIG. 1. $F(v, r) = 0$ and $\mu = 4$, $\lambda = 1$.

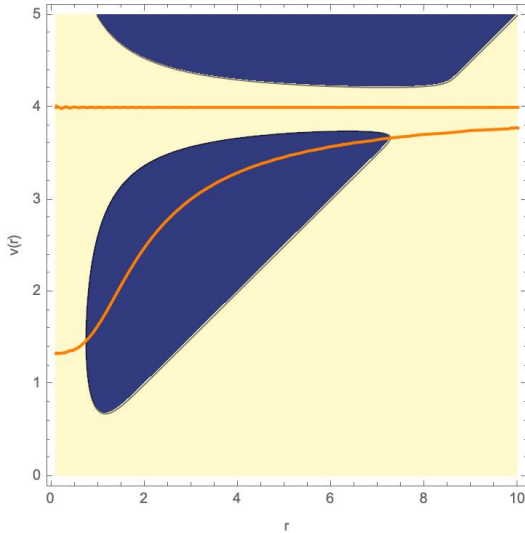


FIG. 2. The same graph as Figure 1, but with $\dot{M} = \frac{dM}{dv} = 0$ (orange line).

(NEC) near the center. As shown in [88], the *outer apparent horizon* is spacelike, while the *inner apparent horizon* is timelike if the NEC horizon is located within the inner horizon.

The *outer horizon* grows, while the *inner horizon* shrinks. At the minimum of the inner horizon, it meets the NEC horizon and becomes spacelike, resulting in two growing horizons. At the maximum of the outer horizon, it becomes null, meets the NEC horizon, and transitions to being timelike. Eventually, the two horizons merge and disappear, leaving behind a *horizonless object with a regular center* for a brief period.

In Figure 2, the evolution of NEC horizons is depicted. The NEC horizon meets the inner horizon at its minimum and the outer horizon at its maximum.

B. Model 2: $k_0 = -1$, $k_1 = k_1(v)$

In this section, we consider a model where the parameters satisfy:

$$\begin{aligned} k_0(v) &= -1, \\ k_1(v) &= k_1(v), \\ k_3(v) &= k_2(v) = 0. \end{aligned} \quad (27)$$

Under these conditions, the mass function takes the form:

$$\begin{aligned} M(v, r) &= -\frac{\rho_0(v)}{8k_1^3(v)} e^{-2k_1(v)r} [1 + 2rk_1(v) + 2r^2k_1^2(v)] \\ &\quad + M_0(v), \end{aligned} \quad (28)$$

where $k_1(v)$ is an arbitrary function of time, and it must satisfy $k_1(v) \neq 0$. This solution generalizes the black hole solution obtained in [87]. Similar to the previous model, we analyze different cases of this spacetime.

1. Regular Black Hole Case: $M_0(v) \equiv \frac{\rho_0(v)}{8k_1^3(v)}$

In this case, the metric (1) with the mass function (28) describes a *dynamical regular black hole*. The Kretschmann scalar at the center $r = 0$ is given by:

$$\lim_{r \rightarrow 0} K = \frac{512}{3} k_1^6(v) M_0^2(v). \quad (29)$$

This ensures that the spacetime curvature remains finite at the core, satisfying the regularity condition.

The energy density ρ and pressure P take the following forms:

$$\begin{aligned} \rho &= 8M_0(v)k_1^3(v)e^{-2k_1(v)r}, \\ P &= 8M_0(v)k_1^3(v)e^{-2k_1(v)r}(-1 + k_1(v)r). \end{aligned} \quad (30)$$

These expressions demonstrate that the energy density and pressure decrease smoothly away from the center, contributing to the regular structure of the black hole.

The weak and dominant energy conditions require the following constraints:

$$\rho_0(v) > 0, \quad (31)$$

$$r \leq \frac{2}{k_1(v)}. \quad (32)$$

These conditions ensure that the matter distribution satisfies physically reasonable energy bounds.

At $r \rightarrow 0$, the solution exhibits a *de Sitter core*, preventing the formation of a singularity. At $r \rightarrow \infty$, the solution smoothly transitions to the *Schwarzschild limit*, ensuring the expected asymptotic flatness.

This model presents an alternative scenario for regular black holes, where the choice of $k_1(v)$ determines the dynamical evolution of the solution.

Under the following choices for the arbitrary functions:

$$\begin{aligned} k_1(v) &= (\mu - v)^2, \\ \rho_1(v) &= 4\lambda k_1^3(v)v, \end{aligned} \quad (33)$$

we can, similar to Model 1, plot the function:

$$F(v, r) = 1 - \frac{2M(v, r)}{r} = 0.$$

In Figure 3, the apparent horizon behavior is illustrated. In Figure 4, the evolution of NEC horizons is depicted.

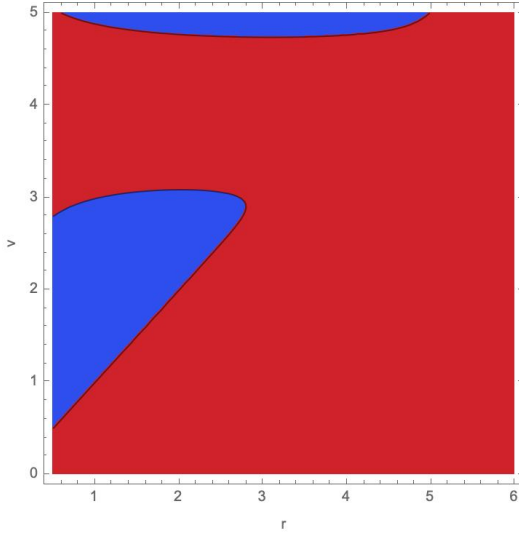


FIG. 3. $F(v, r) = 0$ for $\mu = 4$, $\lambda = 1$.

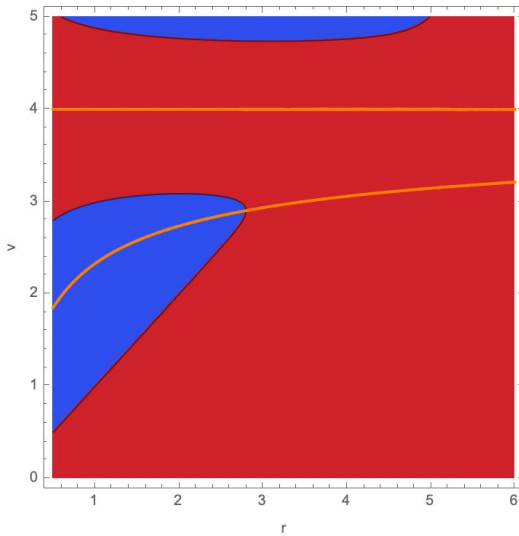


FIG. 4. Same graph as Figure 3, but with $\dot{M} = 0$.

III. MATCHING THE INTERIOR AND EXTERIOR SOLUTIONS

While the solutions (21) and (28) describe a regular center, they are generally valid only in the vicinity of the center. Even though these solutions correspond to known models [86, 87], a more realistic approach would be to match these solutions to an exterior spacetime representing collapsing matter with a physically realistic equation of state.

The simplest dynamical exterior solution is the Vaidya metric, but matching in this case is only possible if the energy density in (21) and (28) vanishes at some radius, which is not observed in our solutions. Instead, we consider a *generalized Vaidya metric*, namely the Husain solution, which corresponds to the barotropic equation of state:

$$P = \alpha\rho.$$

The mass function is given by [89, 90]:

$$M(v, r) = M_1(v) + \rho_1 r^{1-2\alpha}. \quad (34)$$

The curvature invariants Ricci scalar (R), squared Ricci scalar (S), and Kretschmann scalar (K) can be expressed in terms of the mass function $M(v, r)$, energy density $\rho(v, r)$, and pressure $P(v, r)$ as:

$$\begin{aligned} R &= 2\rho - 2P, \\ S &= 2\rho^2 + 2P^2, \end{aligned} \quad (35)$$

$$K = \frac{48M^2}{r^6} - \frac{16M}{r^3} (2\rho - P) + 8\rho^2 - 8\rho P + 4P^2.$$

These expressions indicate that for a smooth matching of all curvature invariants, it is sufficient to match the mass function $M(v, r)$, the energy density $\rho(v, r)$, and the pressure $P(v, r)$ at the matching hypersurface.

A. Dymnikova Solution

Let us first consider the solution (21), which corresponds to the *dynamical Dymnikova black hole solution*. Since we are focusing on regular black hole solutions, we must ensure the matching conditions hold.

From the expressions for energy density and pressure (23), we observe that, in terms of k_0 and k_3 , the equation of state takes the form:

$$P = \rho \left(\frac{M_0 k_3}{6} - 1 \right). \quad (36)$$

This equation of state behaves like a *barotropic equation of state* $P = \alpha\rho$ at a specific matching radius $r = r_b$, where:

$$r_b^3 = \frac{6(\alpha + 1)}{k_3}. \quad (37)$$

We will use this matching radius r_b to match the *interior Dymnikova solution* with the *exterior Husain solution*.

B. Husain Solution

In the Husain solution, the energy density is given by:

$$\rho_{\text{Husain}} = 2(1 - 2\alpha) \frac{\rho_1(v)}{r^{2\alpha+2}}. \quad (38)$$

To ensure a smooth transition between the two solutions at the hypersurface $r = r_b$, we must match the energy densities and pressures at this radius.

This approach provides a physically consistent model where the regular interior solution transitions smoothly into an exterior generalized Vaidya spacetime, allowing for a realistic description of a collapsing regular black hole.

The energy density from the Husain solution (38) matches the energy density of the Dymnikova-like solution (23) if:

$$\rho_1(v) = \frac{M_0(v)}{3(1 - 2\alpha)} r_b^{2\alpha+2} e^{-\frac{2(\alpha+1)}{3}}. \quad (39)$$

Similarly, the mass function in (21) transitions smoothly to the Husain mass function (34) at $r = r_b$ if:

$$M_1(v)|_{r=r_b} = M_0(v) \left(1 - \frac{3}{1 - 2\alpha} e^{-\frac{2(\alpha+1)}{3}} \right). \quad (40)$$

Thus, the metric tensor, energy density, and pressure of solutions (21) and (34) are equal at $r = r_b$ if conditions (39) and (40) hold. This confirms that the Husain solution can describe the gravitational collapse leading to a regular black hole formation.

We now apply the same method to match the regular black hole solution (28) with the Husain solution (34). From the energy density (30), the equation of state follows:

$$P = (k_1 r - 1)\rho. \quad (41)$$

This behaves like a barotropic equation of state $P = \alpha\rho$ at the matching radius $r = r_b$, where:

$$r_b = \frac{\alpha + 1}{k_1}. \quad (42)$$

At this radius, the energy density (30) transforms into the Husain energy density (38) if:

$$\rho_1 = \frac{4M_0 k_1^3}{1 - 2\alpha} r_b^{2\alpha+2} e^{-2(\alpha+1)}. \quad (43)$$

Additionally, the *mass function* in (28) transitions to the Husain solution (34) at $r = r_b$ if the condition:

$$M_1 = M_0 \left(1 - \frac{9 + 6\alpha + 5\alpha^2 + 2\alpha^3}{1 - 2\alpha} e^{-2(\alpha+1)} \right) \quad (44)$$

is satisfied.

Ensuring these conditions, the dynamical collapse of the Husain solution leads to the formation of a regular black hole with a smooth transition from the interior to the exterior spacetime.

The solution (28) is successfully matched with the *Husain solution* (34) at the hypersurface $r = r_b$ (as defined in (42)) if the conditions (43) and (44) hold.

It is important to note that, in this case, matching solution (28) with the standard Vaidya spacetime is not possible because, for any $r > 0$, the energy density of the Husain solution remains nonzero:

$$\rho_{\text{Husain}} \neq 0. \quad (45)$$

If one opts to use the Vaidya spacetime as an exterior solution for these metrics, it would be necessary to introduce a thin matter layer at the matching hypersurface. In this case: The interior solutions (21) or (28) must be matched with a Vaidya spacetime. A thin matter layer would be required at the matching interface to account for the discontinuity in the energy density.

However, performing such a matching lies beyond the scope of this paper, so we do not explore this possibility further in the current study.

IV. SHADOW PROPERTIES

When one opts for observation features of obtained solutions, then one should investigate shadow properties of external Husain solution. One can calculate dynamical shadow of Husain solution (34) the method of which has been developed in the paper [91], however, this method properly works for slowly evolving systems and it is not applicable for gravitational collapse. On this reason, one can calculate the black hole shadow of static Husain solution which corresponds to the case when black hole has been already formed. This metric has the following form

$$ds^2 = - \left(1 - \frac{2M}{r} + \frac{J}{r^{2\alpha}} \right) dt^2 + \left(1 - \frac{2M}{r} + \frac{J}{r^{2\alpha}} \right)^{-1} dr^2 + r^2 d\Omega^2 \quad (46)$$

here M is mass of a black hole, J is a parameter associated with properties of baryonic matter ($J = Q^2$ for $\alpha = 1$ and the metric becomes Reissner-Nordstrom spacetime). α is a parameter of equation of state $P = \alpha\rho$. To satisfy all energy conditions one should demand the following conditions to be held:

$$\begin{aligned} \alpha &\in [-1, 1], \quad \alpha \neq \frac{1}{2}, \\ J &\leq M, \quad J > 0 \text{ if } \alpha > \frac{1}{2}. \end{aligned} \quad (47)$$

The shadow radius is calculated as follows [32]

$$R_{sh} = \frac{r_{ph}}{\sqrt{f(r_{ph})}}, \quad (48)$$

where the photon sphere radius is calculated by solving this relation for r_{ph} :

$$f'(r_{ph})r_{ph} = 2f(r_{ph}). \quad (49)$$

α	r_{ph}	R_{sh}
0	2.0	3.16228
1	2.61803	4.09982
2	2.94104	4.45682
3	2.99165	4.49533
4	2.99885	4.49948
5	2.99985	4.49994
6	2.99998	4.49999

TABLE I. Photon sphere radius (r_{ph}) and shadow radius (r_{sh}) for different values of α with constant $M = 1$ and $J = 0.5$.

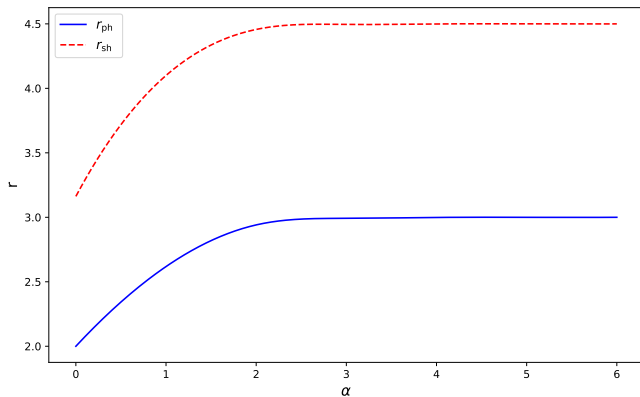


FIG. 5. Figure shows the shadow radius and photon sphere radius versus α .

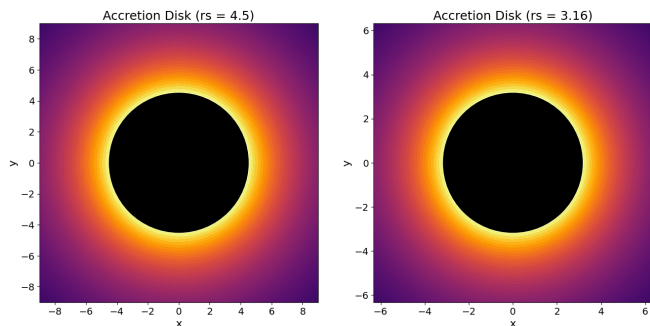


FIG. 6. Figure shows the spherical accretion disk around black hole for different shadow radii.

From Table I and Figures 5, 6, we observe that as the parameter α increases, both the photon sphere radius r_{ph} and the shadow radius R_{sh} increase monotonically. When $\alpha = 0$, corresponding to the baseline scenario, the photon sphere lies at $r_{\text{ph}} = 2.0$ and the shadow radius is $R_{\text{sh}} \approx 3.16228$. As α grows, the most substantial changes occur for moderate values $1 \leq \alpha \leq 3$, after which both radii begin to saturate around $r_{\text{ph}} \approx 3.0$ and $R_{\text{sh}} \approx 4.5$. Physically, a larger photon sphere and shadow radius imply enhanced light bending, allowing photons to orbit at larger radii and causing a more extended dark region, or “silhouette, as seen by a distant observer. The near-constant values for $\alpha \geq 4$ suggest an asymptotic regime in which further increases in α have diminishing effects on the geometry, pointing to a limiting

configuration for the underlying spacetime model.

V. DISCUSSIONS

In this section, we analyze the obtained solutions and the constraints they must satisfy. Our discussion primarily focuses on the solution:

$$M(v, r) = M_0(v) \left(1 - e^{-\frac{1}{9} k_3(v) r^3} \right), \quad (50)$$

though the conclusions drawn here also apply to the second model.

One of the key observations is that when the function $k_3(v)$ increases, the energy conditions remain valid, and the black hole possesses two apparent horizons: Outer apparent horizon: Spacelike and increasing. Inner apparent horizon: Timelike and shrinking.

This behavior follows from the condition:

$$\dot{M} = \dot{M}_0 - \dot{M}_0 e^{-k_3 r^3} + \dot{k}_3 M_0 r^3 e^{-k_3 r^3} \geq 0. \quad (51)$$

However, the dynamics change dramatically when $k_3(v)$ starts decreasing. In this case: The energy conditions are violated, and the structure of the apparent horizons changes when the NEC horizon crosses one of the apparent horizons. The region of energy condition violation expands and extends to infinity as $k_3(v) \rightarrow 0$. At this point, the apparent horizons merge and disappear. However, as shown in the figures, they reappear later, with the outer apparent horizon growing and the inner horizon shrinking. This happens because when the horizons reappear, the energy conditions are no longer violated.

As an example, we consider a mass function of the form:

$$M(v, r) = M_0(v) - M_0(v) e^{-r^3 \sin^2 v}. \quad (52)$$

This type of function illustrates the periodic nature of horizon formation and disappearance. The apparent horizon behavior is depicted in Figures 7 and 8.

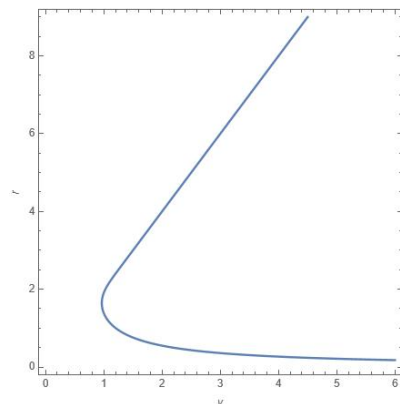


FIG. 7. Apparent horizon evolution with a linear $k_3(v)$.

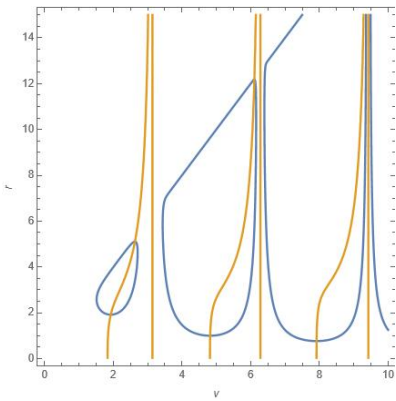


FIG. 8. Apparent horizon evolution with an oscillatory $k_3(v)$.

These plots reveal an infinite sequence of black holes that: Initially grow, Start evaporating, Disappear and then Reappear after a short time. This effect occurs because the function $k_3(v)$ vanishes at an infinite number of points. The vertical lines in the Figures 7 and 8 indicate the zeros of $k_3(v)$, where the black hole disappears.

Despite this intriguing behavior, we have not found a reasonable physical mechanism that could explain this continuous formation and disappearance of black holes. Furthermore, we argue that it is not meaningful to consider black hole evolution beyond the first moment when $k_3(v)$ becomes zero.

The reason for this is that when $k_3(v) = 0$: A jump of the second kind occurs. The entire spacetime, which previously exhibited widespread energy condition violations, suddenly transitions into a region where energy conditions are no longer violated.

Since such a transition is not physically plausible, we conclude that: The evolution of the system must stop at the first instance when $k_3(v) = 0$. Any further continuation beyond this point would be unphysical. This requirement imposes an important constraint on our model, ensuring that the evolution remains physically meaningful and does not lead to unexplainable behavior.

VI. CONCLUSIONS

The obtained solutions (21) and (28) describe a regular black hole, demonstrating the possibility of avoiding singularity formation. However, these solutions have an essential drawback: the pressure increases as a function of the radial coordinate r . This behavior presents two significant issues: In a physically realistic model, the pressure should not increase as we move toward the outer regions of the collapsing star. Dominant Energy Condition (DEC) Violation: At a certain radius $r = r_{\text{violation}}$, the dominant energy condition is violated, signaling the need for an external matching.

Moreover, solutions (21) and (28) were derived based on an expansion of the equation of state coefficient $k(v, r)$ in

the neighborhood of the center. As a result, these solutions are only valid near the regular center and cannot be used to describe the entire spacetime. Thus, a matching with an external solution is required to construct a complete dynamical black hole model.

The simplest metric that describes dynamical black holes is the Vaidya metric. However, a smooth transition between the interior solutions (21), (28), and the Vaidya metric would require an additional thin matter layer, complicating the problem and making the model more artificial.

A more natural and physically motivated choice is to assume that the solutions (21) and (28) arise due to critical compression of ordinary baryonic matter during gravitational collapse. This assumption implies that the exterior geometry must be a dynamical black hole solution with a barotropic equation of state $P = \alpha\rho$.

Such a solution is already known in the literature as the Husain solution [89]. We have successfully matched the obtained solutions (21) and (28) with the Husain metric and demonstrated that the gravitational collapse of baryonic matter can lead to the formation of a regular center.

To explore observational signatures of these solutions, we investigated the black hole shadow, discarding the static Husain solution. However, despite the above analysis, it remains unclear whether a regular center is always formed or if gravitational collapse can still end in a singularity. From Table I and Figures 5, 6, we observe that as the parameter α increases: Both the photon sphere radius r_{ph} and the shadow radius R_{sh} increase monotonically. The resulting shadow images could support either a regular black hole model or a singular one.

Matching the interior and exterior solutions suggests the occurrence of a phase transition in the collapsing matter. Since this transition occurs during gravitational collapse and the formation of apparent horizons may be delayed, further investigation is required to: Identify the physical mechanisms contributing to this phase transition. Study possible observational signatures of this transition.

At the moment of phase transition, an energy flux should be emitted, which may be detectable. Understanding the nature of this flux requires: Considering quantum effects in the collapse process. Estimating the power and observational properties of the emitted energy flux. Future work should focus on these aspects to determine whether the final state of collapse results in a truly regular black hole or a singularity.

ACKNOWLEDGMENTS

A. Ö. would like to acknowledge the contribution of the COST Action CA21106 - COSMIC WISPerS in the Dark Universe: Theory, astrophysics and experiments (CosmicWISPerS), the COST Action CA22113 - Fundamental challenges in theoretical physics (THEORY-CHALLENGES) and CA23130 - Bridging high and low energies in search of quantum gravity (BridgeQG). We also thank TUBITAK and SCOAP3 for their support.

- [1] R. Penrose, *Phys. Rev. Lett.* **14**, 57 (1965).
- [2] R. Penrose, *Riv. Nuovo Cim.* **1**, 252 (1969).
- [3] S. W. Hawking and R. Penrose, *Proc. Roy. Soc. Lond. A* **314**, 529 (1970).
- [4] K. Akiyama *et al.* (Event Horizon Telescope), *Astrophys. J. Lett.* **875**, L1 (2019), arXiv:1906.11238 [astro-ph.GA].
- [5] K. Akiyama *et al.* (Event Horizon Telescope), *Astrophys. J. Lett.* **930**, L12 (2022), arXiv:2311.08680 [astro-ph.HE].
- [6] F. Koyuncu and O. Dönmez, *Mod. Phys. Lett. A* **29**, 1450115 (2014).
- [7] O. Donmez, F. Dogan, and T. Sahin, *Universe* **8**, 458 (2022), arXiv:2205.14382 [astro-ph.HE].
- [8] O. Donmez, *Res. Astron. Astrophys.* **24**, 085001 (2024), arXiv:2310.13847 [astro-ph.HE].
- [9] E. B. Gliner, *Soviet Journal of Experimental and Theoretical Physics* **22**, 378 (1966).
- [10] A. D. Sakharov, *Soviet Journal of Experimental and Theoretical Physics* **22**, 241 (1966).
- [11] J. Bardeen, in *Proceedings of the 5th International Conference on Gravitation and the Theory of Relativity* (1968) p. 87.
- [12] E. Ayon-Beato and A. Garcia, *Phys. Rev. Lett.* **80**, 5056 (1998), arXiv:gr-qc/9911046.
- [13] E. Ayon-Beato and A. Garcia, *Gen. Rel. Grav.* **31**, 629 (1999), arXiv:gr-qc/9911084.
- [14] S. A. Hayward, *Phys. Rev. Lett.* **96**, 031103 (2006), arXiv:gr-qc/0506126.
- [15] Y. Verbin, B. Pulice, A. Övgün, and H. Huang, (2024), arXiv:2412.20989 [gr-qc].
- [16] D. P. Sorokin, *Fortsch. Phys.* **70**, 2200092 (2022), arXiv:2112.12118 [hep-th].
- [17] L. Balart, G. Panotopoulos, and A. Rincón, *Fortsch. Phys.* **71**, 2300075 (2023), arXiv:2309.01910 [gr-qc].
- [18] M. Okyay and A. Övgün, *JCAP* **01**, 009 (2022), arXiv:2108.07766 [gr-qc].
- [19] K. A. Bronnikov, *Phys. Rev. D* **63**, 044005 (2001), arXiv:gr-qc/0006014.
- [20] K. A. Bronnikov, V. N. Melnikov, and H. Dehnen, *Gen. Rel. Grav.* **39**, 973 (2007), arXiv:gr-qc/0611022.
- [21] K. A. Bronnikov, *Phys. Rev. D* **96**, 128501 (2017), arXiv:1712.04342 [gr-qc].
- [22] G. Denardo and R. Ruffini, *Phys. Lett. B* **45**, 259 (1973).
- [23] O. B. Zaslavskii, *Mod. Phys. Lett. A* **36**, 2150120 (2021), arXiv:2006.02189 [gr-qc].
- [24] V. Vertogradov, *Commun. Theor. Phys.* **75**, 045404 (2023), arXiv:2210.04784 [gr-qc].
- [25] V. Vertogradov, (2025), arXiv:2501.13739 [gr-qc].
- [26] A. Bonanno, D. Malafarina, and A. Panassiti, *Phys. Rev. Lett.* **132**, 031401 (2024), arXiv:2308.10890 [gr-qc].
- [27] M. Misyura, A. Rincon, and V. Vertogradov, (2024), arXiv:2405.05370 [gr-qc].
- [28] R. V. Konoplich, S. G. Rubin, A. S. Sakharov, and M. Y. Khlopov, *Phys. Atom. Nucl.* **62**, 1593 (1999).
- [29] M. Y. Khlopov, R. V. Konoplich, S. G. Rubin, and A. S. Sakharov, *Grav. Cosmol.* **2**, S1 (1999), arXiv:hep-ph/9912422.
- [30] M. Y. Khlopov, *Res. Astron. Astrophys.* **10**, 495 (2010), arXiv:0801.0116 [astro-ph].
- [31] P. Nicolini, A. Smailagic, and E. Spallucci, *Phys. Lett. B* **632**, 547 (2006), arXiv:gr-qc/0510112.
- [32] S. Vagnozzi *et al.*, *Class. Quant. Grav.* **40**, 165007 (2023), arXiv:2205.07787 [gr-qc].
- [33] K. M. Belotsky, A. D. Dmitriev, E. A. Esipova, V. A. Gani, A. V. Grobov, M. Y. Khlopov, A. A. Kirillov, S. G. Rubin, and I. V. Svadkovsky, *Mod. Phys. Lett. A* **29**, 1440005 (2014), arXiv:1410.0203 [astro-ph.CO].
- [34] I. Dymnikova and M. Khlopov, *Int. J. Mod. Phys. D* **24**, 1545002 (2015), arXiv:1510.01351 [gr-qc].
- [35] I. Dymnikova, *Gen. Rel. Grav.* **24**, 235 (1992).
- [36] C. Bambi and L. Modesto, *Phys. Lett. B* **721**, 329 (2013), arXiv:1302.6075 [gr-qc].
- [37] I. Dymnikova, *Class. Quant. Grav.* **19**, 725 (2002), arXiv:gr-qc/0112052.
- [38] M. Molina and J. R. Villanueva, *Class. Quant. Grav.* **38**, 105002 (2021), arXiv:2101.07917 [gr-qc].
- [39] M. Azreg-Ainou, *Phys. Lett. B* **730**, 95 (2014), arXiv:1401.0787 [gr-qc].
- [40] S. H. Mazharimousavi and M. Halilsoy, *Phys. Lett. B* **796**, 123 (2019).
- [41] M. Halilsoy, A. Ovgun, and S. H. Mazharimousavi, *Eur. Phys. J. C* **74**, 2796 (2014), arXiv:1312.6665 [gr-qc].
- [42] L. C. N. Santos, *Eur. Phys. J. C* **84**, 1318 (2024), arXiv:2411.18804 [gr-qc].
- [43] R. Carballo-Rubio *et al.*, (2025), arXiv:2501.05505 [gr-qc].
- [44] K. Sueto and H. Yoshino, *PTEP* **2023**, 103E01 (2023), arXiv:2301.10456 [gr-qc].
- [45] A. Övgün, *Phys. Rev. D* **99**, 104075 (2019), arXiv:1902.04411 [gr-qc].
- [46] A. Övgün, R. C. Pantig, and A. Rincón, *Annals Phys.* **463**, 169625 (2024), arXiv:2402.14190 [gr-qc].
- [47] A. A. Araújo Filho, *JCAP* **01**, 072 (2025), arXiv:2410.23165 [gr-qc].
- [48] N. Heidari, A. A. Araújo Filho, R. C. Pantig, and A. Övgün, *Phys. Dark Univ.* **47**, 101815 (2025), arXiv:2410.08246 [gr-qc].
- [49] A. A. A. Filho, J. R. Nascimento, A. Y. Petrov, P. J. Porfírio, and A. Övgün, *Phys. Dark Univ.* **46**, 101630 (2024), arXiv:2406.12015 [gr-qc].
- [50] A. Bokulic, E. Franzin, T. Juric, and I. Smolic, *Phys. Lett. B* **854**, 138750 (2024), arXiv:2311.17151 [gr-qc].
- [51] A. Abdujabbarov, M. Amir, B. Ahmedov, and S. G. Ghosh, *Phys. Rev. D* **93**, 104004 (2016), arXiv:1604.03809 [gr-qc].
- [52] Z. Feng, Y. Ling, X. Wu, and Q. Jiang, *Sci. China Phys. Mech. Astron.* **67**, 270412 (2024), arXiv:2308.15689 [gr-qc].
- [53] A. Allahyari, M. Khodadi, S. Vagnozzi, and D. F. Mota, *JCAP* **02**, 003 (2020), arXiv:1912.08231 [gr-qc].
- [54] S. Fernando and J. Correa, *Phys. Rev. D* **86**, 064039 (2012), arXiv:1208.5442 [gr-qc].
- [55] B. Kleihaus, J. Kunz, F. Navarro-Lerida, and U. Neemann, *Gen. Rel. Grav.* **40**, 1279 (2008), arXiv:0705.1511 [gr-qc].
- [56] B. Kleihaus, J. Kunz, A. Sood, and M. Wirschins, *Phys. Rev. D* **58**, 084006 (1998), arXiv:hep-th/9802143.
- [57] B. Toshmatov, Z. Stuchlík, and B. Ahmedov, *Phys. Rev. D* **95**, 084037 (2017), arXiv:1704.07300 [gr-qc].
- [58] Z. Stuchlík and J. Schee, *Eur. Phys. J. C* **79**, 44 (2019).
- [59] M. Sharif and A. Khan, *Mod. Phys. Lett. A* **37**, 2250049 (2022).
- [60] M. Sharif and W. Javed, *J. Korean Phys. Soc.* **57**, 217 (2010), arXiv:1007.4995 [gr-qc].

- [61] S. Hod, *Phys. Rev. D* **109**, 064074 (2024), [arXiv:2401.07907 \[gr-qc\]](#).
- [62] O. B. Zaslavskii, *Phys. Lett. B* **688**, 278 (2010), [arXiv:1004.2362 \[gr-qc\]](#).
- [63] R. Kumar, S. G. Ghosh, and A. Wang, *Phys. Rev. D* **100**, 124024 (2019), [arXiv:1912.05154 \[gr-qc\]](#).
- [64] R. Kumar, A. Kumar, and S. G. Ghosh, *Astrophys. J.* **896**, 89 (2020), [arXiv:2006.09869 \[gr-qc\]](#).
- [65] R. Kumar Walia, S. G. Ghosh, and S. D. Maharaj, *Astrophys. J.* **939**, 77 (2022), [arXiv:2207.00078 \[gr-qc\]](#).
- [66] S. Murk and I. Soranidis, *Phys. Rev. D* **108**, 044002 (2023), [arXiv:2304.05421 \[gr-qc\]](#).
- [67] S. G. Ghosh and S. D. Maharaj, *Eur. Phys. J. C* **75**, 7 (2015), [arXiv:1410.4043 \[gr-qc\]](#).
- [68] W. L. Smith and R. B. Mann, *Phys. Rev. D* **58**, 124021 (1998), [arXiv:gr-qc/9806013](#).
- [69] S. Ansoldi, in *Conference on Black Holes and Naked Singularities* (2008) [arXiv:0802.0330 \[gr-qc\]](#).
- [70] C. Lan, H. Yang, Y. Guo, and Y.-G. Miao, *Int. J. Theor. Phys.* **62**, 202 (2023), [arXiv:2303.11696 \[gr-qc\]](#).
- [71] Y. Zhang, Y. Zhu, L. Modesto, and C. Bambi, *Eur. Phys. J. C* **75**, 96 (2015), [arXiv:1404.4770 \[gr-qc\]](#).
- [72] F. Shojai, A. Sadeghi, and R. Hassannejad, *Class. Quant. Grav.* **39**, 085003 (2022), [arXiv:2202.14024 \[gr-qc\]](#).
- [73] K. Mosani and P. S. Joshi, (2023), [arXiv:2306.04298 \[gr-qc\]](#).
- [74] P. Bueno, P. A. Cano, R. A. Hennigar, and A. J. Murcia, (2024), [arXiv:2412.02742 \[gr-qc\]](#).
- [75] P. Bueno, P. A. Cano, R. A. Hennigar, and A. J. Murcia, (2024), [arXiv:2412.02740 \[gr-qc\]](#).
- [76] M. D. Mkenyeleye, R. Goswami, and S. D. Maharaj, *Phys. Rev. D* **90**, 064034 (2014), [arXiv:1407.4309 \[gr-qc\]](#).
- [77] V. Vertogradov, *Int. J. Mod. Phys. A* **33**, 1850102 (2018), [arXiv:2210.16131 \[gr-qc\]](#).
- [78] V. Vertogradov, *Universe* **6**, 155 (2020), [arXiv:2209.10976 \[gr-qc\]](#).
- [79] V. Vertogradov, (2022), [10.33910/2687-153X-2022-4-1-17-23](#), [arXiv:2211.16189 \[gr-qc\]](#).
- [80] V. Vertogradov, *Gen. Rel. Grav.* **56**, 59 (2024), [arXiv:2311.15671 \[gr-qc\]](#).
- [81] Y. Heydarzade and V. Vertogradov, *Eur. Phys. J. C* **84**, 582 (2024), [arXiv:2311.08930 \[gr-qc\]](#).
- [82] V. Vertogradov and M. Misyura, *Universe* **8**, 567 (2022), [arXiv:2209.07441 \[gr-qc\]](#).
- [83] L. Herrera, A. Di Prisco, and J. Ospino, *Phys. Rev. D* **74**, 044001 (2006), [arXiv:gr-qc/0609009](#).
- [84] V. Vertogradov and D. Kudryavcev, *Mod. Phys. Lett. A* **38**, 2350119 (2023), [arXiv:2212.07130 \[gr-qc\]](#).
- [85] G. Manna, P. Majumdar, and B. Majumder, *Phys. Rev. D* **101**, 124034 (2020), [arXiv:1909.07224 \[gr-qc\]](#).
- [86] I. Dymnikova, *Gen. Rel. Grav.* **24**, 235 (1992).
- [87] V. Vertogradov and A. Övgün, *Class. Quant. Grav.* **42**, 025024 (2025), [arXiv:2408.02699 \[gr-qc\]](#).
- [88] V. Vertogradov, (2024), [arXiv:2410.10582 \[gr-qc\]](#).
- [89] V. Husain, *Phys. Rev. D* **53**, 1759 (1996), [arXiv:gr-qc/9511011](#).
- [90] V. D. Vertogradov, *Grav. Cosmol.* **22**, 220 (2016).
- [91] V. Vertogradov and A. Övgün, (2024), [arXiv:2412.10930 \[gr-qc\]](#).